TOWARDS SMALL OBJECT DETECTION IN SPACE: PHOTONIC INTEGRATED QUANTUM ILLUMINATION

Isabel Carnoto Amat[1], Jessica César Cuello[1], Rosa María Pulido Puerto[2], Francisco Javier Morales Comalat[2], Pablo Fajardo[1], Luis Enrique García Muñoz[1]

[1]Universidad Carlos III de Madrid (UC3M). Leganés, Spain.
icarnoto@ing.uc3m.es jecesarc@ing.uc3m.es pfajardo@ing.uc3m.es legarcia@ing.uc3m.es
[2]Ingeniería de Sistemas para la Defensa de España (ISDEFE). Madrid, Spain.
rmpulido@isdefe.es fjmorales@isdefe.es

ABSTRACT

This work proposes leveraging quantum mechanical properties for enhanced detection of faint space debris and potentially ill-intentioned small satellites. Central to our system is the design of a Photonic Integrated whispering gallery mode resonator (WGMR), utilizing thin film lithium niobate technology. This resonator serves as an optical−sub-terahertz entanglement source and frequency upconversion stage, ideal for space applications because of its reduced SWaP. Although quantum technologies may not yet be mature for immediate deployment, some expected advancements include improved sensitivity and precision, reduced noise levels, and increased reliability. Leveraging the features of Photonic Integrated WGMR and passive cooling, our design presents a compelling solution for the challenges of weak signal power detection. However, it is crucial to acknowledge that overcoming current limitations, such as achieving higher upconversion efficiency and enhancing the Q factor, requires continued research and development efforts.

KEYWORDS

Quantum illumination, photonic integrated circuit, space debris, entanglement, frequency upconversion.

1. INTRODUCTION

Space debris represent a significant threat to satellites and spacecraft in Earth's orbit due to increasing congestion, raising the risk of collisions with potentially catastrophic outcomes. Monitoring CubeSats and small satellites is essential for security, given the surge in launches and the growing number of satellites, including those from potentially ill-intentioned actors. Accurate detection of both space debris and small satellites is crucial for defence applications; however, current detection methods face limitations due to factors such as debris volume and the size of objects being tracked.

The purpose of this paper is to outline an innovative approach to detecting faint space debris and small satellites by leveraging quantum mechanical properties, particularly the exploitation of entangled photons to enhance detection capabilities. Our objective is to achieve comprehensive coverage of the space environment through the integration of quantum and classical radar systems. The quantum detection component is specifically tailored to detect small debris and satellites at closer ranges, benefiting from heightened sensitivity and noise reduction. Meanwhile, the classical radar system complements this by detecting larger debris at greater distances.

Central to our proposed system is the design and characterization of a compact Photonic Integrated whispering gallery mode resonator, utilizing thin film lithium niobate ($LiNbO_3$)

technology, serving as an optical−sub-terahertz entanglement source and frequency upconversion stage, making it highly suitable for space applications like satellite deployment.

2. State of the Art

Existing space debris detection relies primarily on classical radar systems and optical telescopes. Ground-based radar systems, such as NASA's Haystack Ultrawideband Satellite Imaging Radar (HUSIR) and Goldstone Orbital Debris Radar (Goldstone), track larger debris in low Earth orbit (LEO) and geostationary orbit (GEO), providing data on debris ranging in size from approximately 5 mm to 2-3 cm in low Earth orbit (LEO). Optical telescopes, like the Eugene Stansbery Meter Class Autonomous Telescope (ES-MCAT), utilize visible or infrared light to observe space objects, effectively tracking larger debris and active satellites with high-resolution imaging capabilities [1].

In recent years, there has been growing interest in leveraging quantum technologies, such as quantum illumination, for defence applications, including space debris detection. Quantum illumination exploits quantum entanglement to improve sensitivity and reduce noise levels, offering enhanced detection capabilities compared to classical radar systems. Zhang et al. [2] demonstrated the first quantum illumination experiment in 2015 at optical frequencies, achieving a 20% improvement in detection error probability exponent compared to classical systems. Similarly, Assouly et al. [3] achieved a 20% performance enhancement over any classical system in 2023 at microwave frequencies.

Although quantum technologies may not yet be mature for immediate deployment in space debris detection, there's strong anticipation that quantum illumination could revolutionize the field. Expected advancements include improved sensitivity and reduced noise levels, enabling precise identification of space debris, even in cluttered environments where classical systems struggle. Quantum illumination also promises enhanced precision in determining object position and size, and increased reliability in adverse conditions. Mounting a quantum illumination system on a satellite can also provide a significant advantage, extending detection capabilities to distances unreachable by ground-based systems.

3. Quantum Illumination System Model

The description of our proposed quantum radar system is based on Quantum Illumination (QI), a quantum protocol for target detection introduced by Lloyd [4]. This concept is graphically presented in Figure 1.

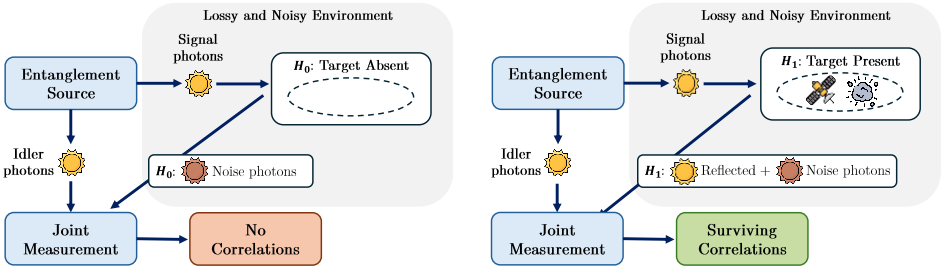

Figure 1. Quantum Illumination protocol. H_0, target absent (left) and H_1, target present (right).

QI involves generating a pair of entangled photons, typically called signal and idler, and sending the signal photon towards the target while retaining the idler as a reference. The transmitted photon is used to probe a distant region where a target may be suspected. If an object is present, the photon may be reflected and received along with the environmental noise photons; otherwise,

only noise photons will be detected. To gain an advantage over classical systems, each received photon must undergo a joint measurement with the idler photon. Even if entanglement is broken due to a lossy and noisy medium, surviving correlations provide information that can be used to probabilistically differentiate between two hypotheses H_0 (target absent) or H_1 (target present) when the process is repeated multiple times [5].

3.1. ELECTRO-OPTIC INTERACTIONS

To first comprehend the functioning of the entanglement source and upconversion stage further proposed, let's first study the interaction between an optical pump (ω_{pump}) and a sub-terahertz field (ω_{sT}) within a medium exhibiting nonlinear characteristics, such as lithium niobate, which will serve as the material for fabricating the photonic integrated circuit.

The nonlinear electro-optic effects induced by the material lead to the modulation of the optical field by the sub-terahertz field, resulting in the generation of two optical sidebands through the processes of Sum Frequency Generation (SFG) and Difference Frequency Generation (DFG) [6]. To enable the interaction between optical and sub-terahertz fields, it suffices to match the sub-terahertz frequency with the optical Free Spectral Range (FSR) of the resonator ($\omega_{sT} = FSR$). This ensures the phase-matching condition is met [7].

In Sum Frequency Generation (SFG), a sub-terahertz and an optical photon are combined to create an up-shifted photon at the sum frequency $\omega_S = \omega_{pump} + \omega_{sT}$, effectively upconverting the sub-terahertz signal into the optical domain. Ideally, the spectrum of this sideband aligns with the input sub-terahertz spectrum, facilitating accurate measurements of the sub-terahertz field once it transitions into the optical domain. On the other hand, in Difference Frequency Generation (DFG), a sub-terahertz photon can stimulate an optical pump photon to decay into a down-shifted optical photon at the difference frequency $\omega_D = \omega_{pump} - \omega_{sT}$, along with an additional sub-terahertz photon ω_{sT}. This process can occur spontaneously without the need for the sub-terahertz signal. This is called spontaneous parametric downconversion (SPDC) and it can be used to generate entangled pairs of sub-terahertz (signal) and optical (idler) photons [8]. We can employ the interaction Hamiltonian, assuming a strong optical pump, to further understand the interactions within the system:

$$\widehat{H}_{int} = \hbar g_0 \sqrt{n_p}\left(\hat{a}_D^{\dagger}\, \hat{a}_{sT}^{\dagger} + \hat{a}_D \hat{a}_{sT}\right) + \hbar g_0 \sqrt{n_p}\left(\hat{a}_S^{\dagger}\, \hat{a}_{sT} + \hat{a}_S\, \hat{a}_{sT}^{\dagger}\right) \quad (1)$$

Where $\hbar$ is the reduced Planck's constant, g_0 the vacuum coupling rate, n_p represents the average number of pump photons, and $\hat{a}_D$, $\hat{a}_S$ and $\hat{a}_{sT}$ are the annihilation operators of the DFG, SFG, and the sub-terahertz modes, respectively.

The first segment, recognized as the two-mode squeezing term, denotes the annihilation of a pump photon, to create a down-shifted optical photon, and a sub-terahertz photon, representing the DFG process. This interaction can generate an entangled two-mode squeezed state between sub-terahertz and optical frequencies. The difference frequency mode will serve as the idler ($\omega_{idler} = \omega_D = \omega_{pump} - FSR$) and the sub-terahertz mode as the signal ($\omega_{signal} = FSR$).

The second segment, labelled the beam splitter term, indicates the annihilation of a pump and a sub-terahertz photon, resulting in an up-shifted optical photon ($\omega_{up} = \omega_{pump} + \omega_{sT}$) corresponding to the SFG process. It showcases an interaction similar to that of a beam splitter, where a photon is eliminated in one mode while another is produced in the other mode, conserving the photon number. As a result, this term can be utilized to transduce photons between modes fundamentally without introducing additional noise.

These two processes, shown in Figure 2, allow us to utilize the same device to generate entangled states and to upconvert the received sub-terahertz signal to the optical domain before the joint measurement. We can choose which process to employ by detuning the optical pump to higher or lower frequencies and matching the sub-terahertz mode to the new required frequency [7].

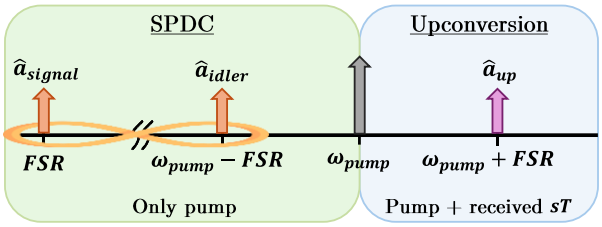

Figure 2. Entanglement generation and upconversion processes diagram in frequency domain.

3.2. Optical– sub-terahertz Photon Entanglement Generation

For entanglement generation, we can detune the pump to a lower frequency, which suppresses the beam splitter interaction responsible for upconversion. Knowing that the thermal populations of the signal (N_{Sth}) and idler (N_{Ith}) modes depend on the modes' frequencies and temperatures according to Planck's thermal radiation equation $N_{j_{TH}} = \frac{1}{e^{\hbar\omega_j/k_BT}-1}$ the two-mode squeezing interaction will produce an entangled two-mode squeezed thermal state with covariance matrix

$$V = \begin{bmatrix} N_S + {}^1/_2 & 0 & N_C & 0 \\ 0 & N_S + {}^1/_2 & 0 & -N_C \\ N_C & 0 & N_I + {}^1/_2 & 0 \\ 0 & -N_C & 0 & N_I + {}^1/_2 \end{bmatrix} \quad (2)$$

Where $N_S = 0.5 \times \left[\cosh(2r)\left(N_{S_{TH}} + N_{I_{TH}} + 1\right) + \left(N_{S_{TH}} - N_{I_{TH}}\right) - 1\right]$, $N_I = 0.5 \times \left[\cosh(2r)\left(N_{S_{TH}} + N_{I_{TH}} + 1\right) - \left(N_{S_{TH}} - N_{I_{TH}}\right) - 1\right]$, $N_C = 0.5 \times \sinh(2r)\left(N_{S_{TH}} + N_{I_{TH}} + 1\right)\cos(\phi)$, r is the squeezing parameter and ϕ the squeezing angle. If we consider working in vacuum conditions ($N_{Sth} = 0$ and $N_{Ith} = 0$), we will obtain an entangled two-mode squeezed vacuum state ($N_S = N_I$) [9], exhibiting the strongest entanglement. This indicates that the higher the frequencies and the lower the temperature, the stronger the entanglement achieved.

3.3. Target Model

The signal photons of the entangled state are employed to probe a region characterized by high losses and a significant thermal background. The objective is to differentiate between our two potential hypotheses, H_0 and H_1, which are assumed to have an equal a priori probability of 50%.

Under H_0, the signal photons are lost, and the radar receives only thermal noise represented as a thermal state with N_T average number of thermal photons. The covariance matrix between the idler and the received thermal photons is:

$$V_0 = \begin{pmatrix} N_T + 1/2 & 0 & 0 & 0 \\ 0 & N_T + 1/2 & 0 & 0 \\ 0 & 0 & N_I + 1/2 & 0 \\ 0 & 0 & 0 & N_I + 1/2 \end{pmatrix} \quad (3)$$

There are no off-diagonal elements in the covariance matrix, which means that there is no correlation between the idler and thermal photons [5].

Under hypothesis H_1, some of the signal photons interact with the target, leading to a blend of reflected photons and thermal noise, forming what we refer to as the return signal. The interaction with the target can be represented by a beamsplitter with extremely low reflectivity $\kappa \ll 1$. One input of the beamsplitter receives the signal, while the other receives a thermal state. The resulting covariance matrix for the idler-return signal is as follows:

$$V_1 = \begin{pmatrix} \kappa N_s + N_T + 1/2 & 0 & \sqrt{\kappa} N_C & 0 \\ 0 & \kappa N_s + N_T + 1/2 & 0 & -\sqrt{\kappa} N_C \\ \sqrt{\kappa} N_C & 0 & N_I + 1/2 & 0 \\ 0 & -\sqrt{\kappa} N_C & 0 & N_I + 1/2 \end{pmatrix} \quad (4)$$

The off-diagonal terms of the matrix are attenuated by the factor $\sqrt{\kappa}$. This reduction, resulting from losses and a noisy channel, may entirely disrupt the initial entanglement. However, the remaining correlations provide us with the chance to differentiate between hypotheses [5].

3.4. Frequency Upconversion and Phase-conjugate Receiver

By detuning to a higher pump frequency, we can suppress the squeezing interaction. The beam splitter interaction facilitates the upconversion of the return photons to the optical domain with a certain efficiency. This enables the use of receivers reliant on photon counting, such as the phase-conjugate receiver proposed by Guha and Erkmen in [10] and shown in Figure 3.

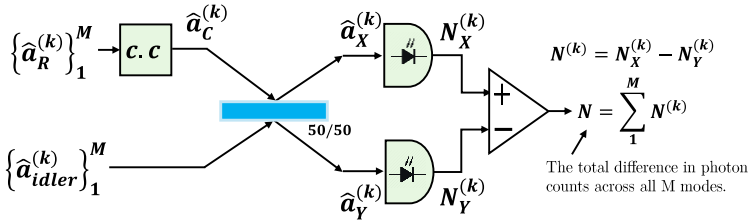

Figure 3. Phase-conjugate receiver [10].

This receiver conducts a joint measurement between the idler and return photons, providing up to a 3dB gain in the SNR compared to the optimal classical receiver when $N_S \ll 1$, $\kappa \ll 1$ and $N_T \gg 1$. Initially, it phase-conjugates the return modes received as $\hat{a}_C = \sqrt{2}\,\hat{a}_V + \hat{a}_R^{\dagger}$, where $\hat{a}_V$ is the vacuum state operator necessary to preserve the commutation relationships. Subsequently, the phase-conjugated signal is interfered with the idler mode in a 50/50 beam splitter, and both outputs are photon-counted and directed into a unitary gain difference amplifier, resulting in the final measurement $N = N_X - N_Y$. With repeated measurements, the number of photons obtained varies as a random variable that can be characterized by the mean and variance N_0 and ${\sigma_0}^2$ under H_0, and N_1 and ${\sigma_1}^2$ under H_1. If the number of entangled states generated M is sufficiently high, the distributions approximate Gaussian distributions with means and variances MN_j and $M{\sigma_j}^2$, respectively. This enables us to convert the problem of distinguishing between two quantum states into distinguishing between two Gaussian distributions using a threshold detector, where $N_{th} = \lceil M(\sigma_1 N_0 + \sigma_0 N_1)/(\sigma_1 + \sigma_0) \rceil$. The detector favors H_0 when $N < N_{th}$ and H_1 otherwise.

4. PIC Design and Characterization

The proposed LiNbO3 photonic integrated circuit was designed to accommodate a pump operating around a wavelength of 1550 nm and a return signal of 500 GHz to 1 THz, to reduce the thermal population as much as possible. It consists of two different subsystems, optical and

sub-terahertz. The optical subsystem includes a bus waveguide, a 50 μm radius ring resonator (RR), and an asymmetric Mach–Zehnder interferometer (AMZI) with a path length imbalance of 250 μm between its two arms. The bus waveguide couples the optical pump to the ring resonator. The optical signal is required within the resonator to enable the generation of entangled pairs of sub-terahertz and optical photons, as well as the upconversion of incoming sub-terahertz photons. This coupling is achieved through evanescent field coupling between the bus waveguide and the cavity. Due to the high Q factor of integrated $LiNbO_3$ resonators, the operational bandwidth of the device is constrained to a few Megahertz (MHz). To increase the bandwidth of the device, a wavelength filter, based on an AMZI, is incorporated. This filter operates by extracting the generated photons in an overcoupled regime (wider resonance), while simultaneously reintroducing the pump into the optical resonator to maintain the highest power possible inside the resonator.

The sub-terahertz system comprises a microstrip antenna for capturing energy from the surrounding space, and a microstrip ring resonator (RR) for confining energy fields within the $LiNbO_3$ RR. Serving as a link between free space and the resonator, the antenna's role is to supply a stable field distribution within the RR.

In the first phase, a passive photonic integrated circuit (PIC) was fabricated. This was used to evaluate the optical elements of the system. Fabricated on a thin-film lithium niobate (TFLN) on-insulator platform, it comprised four AMZIs, each with different gaps between the waveguides of the directional couplers: $AMZI_1$: 0.65 μm, $AMZI_2$: 0.55 μm, $AMZI_3$: 0.45 μm and $AMZI_4$: 0.35 μm. The objective was to determine the gap that yielded a 50/50 splitting ratio in the directional couplers. Additionally, the PIC included eight ring resonators (RRs), each with a varied gap between the input waveguide and the resonator: RR_1: 1.4 μm, RR_2: 1.26 μm, RR_3: 1.11 μm, RR_4: 0.97 μm, RR_5: 0.829 μm, RR_6: 0.686 μm, RR_7: 0.543 μm and RR_8: 0.4 μm. This variation aimed to characterize the transmission spectrum of the resonator relative to the gap.

The second phase involved the fabrication of the complete system in a PIC, therefore, including now the sub-terahertz subsystem. Six structures were fabricated, adjusting the gap between the bus waveguide and resonator, as well as the gap in the directional couplers, around the optimal values determined in the prior fabrication round. This second PIC has yet to undergo characterization; hence, in this manuscript, we only present the characterization results of the first PIC. In Figure 4 we illustrate the design of the complete system, the footprint of the PIC compared to a coin, alongside microscope images of the first and second photonic integrated circuits.

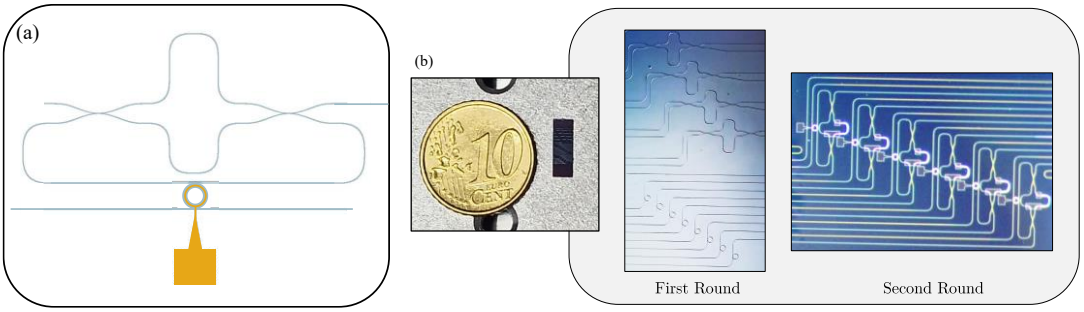

Figure 4. (a) PIC design and (b) microscope images of the first and second fabrication rounds.

In Figure 5, we present the measurements of the most effective structures, namely $AMZI_3$ and resonators six, seven and eight. Figure 5 (left) illustrates the optical response obtained at both arms of the interferometer when light is injected through its top input arm. We achieved an extinction ratio (ER) of 25 dB and a Free Spectral Range (FSR) of 662.5 ± 37.5 GHz. The ER

achieved ensures that minimal pump power appears at the output port along with the generated sidebands, ensuring that almost all the pump power is reinjected into the cavity. The FSR matches the frequency range of our intended application. Figure 5 (right) shows the transmission spectrums of resonators RR_6, RR_7 and RR_8. From these results we can conclude that the optimum gap between the input waveguide and the ring resonator is around 0.543 µm (RR_7) due to its flat spectrum. By performing a Lorentzian fit, we estimate an intrinsic quality factor of $Q = 10^5$.

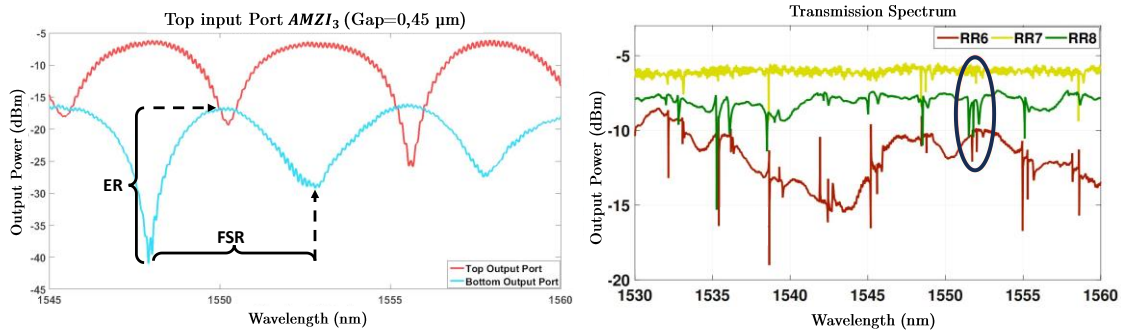

Figure 5. Espectral response of $AMZI_3$ (left) and RR_6, RR_7 and RR_8 (right).

5. QUANTUM ILLUMINATION DETECTION SYSTEM

In Figure 6 we illustrate a block diagram outlining the design and expected operation. Step 1 involves pumping with a detuned-down pump to suppress beamsplitter interaction. This pumping will generate pairs of entangled photons via SPDC, obtained at point 2. The idler photons must be stored in a structure with minimal losses, such as a resonator or low-loss delay line, while the signal photons are transmitted to probe a section of space. If a target exists, the photons may reflect and be received by the antenna along with thermal noise from the environment, as indicated in step 3. At this point, the pump will switch to a detuned-up position to suppress squeezing operation. This pump will enable the upconversion of received photons to the optical spectrum. The upconverted photons obtained at point 5 are then sent along with the stored idler photons to point 6, the phase-conjugate receiver, where they interfere with each other and are then photon counted to ultimately obtain statistics providing information about our potential target.

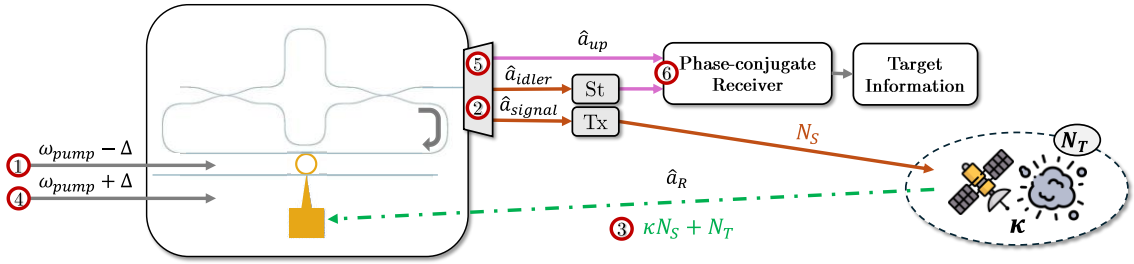

Figure 6. Block diagram of full PI small object detection system based on QI.

6. CONCLUSION

The goal of this research is to outline a design for a quantum illumination small object detection system with particular focus on the design of a photonic integrated whispering gallery mode resonator, utilizing thin film lithium niobate that would work as a sub-terahertz-optical photons entanglement source as well as a frequency upconversion stage for the received photons. Utilizing a whispering gallery mode PIC allows for an extended interaction time with the nonlinear material without requiring an excessively large crystal, thus ensuring lower losses. Furthermore,

employing a resonator scheme enables higher levels of intracavity power compared to the pump power and facilitates a reduction in SWaP (size, weight, and power consumption). These characteristics make this design highly appealing for spaceborne applications, as it offers a compact SWaP profile, simplified connectivity, and minimal power demands. Notably, quantum illumination proves advantageous only in scenarios characterized by weak signal power, which is crucial for spaceborne applications where power is a limited resource. Another key characteristic of this design is radiative passive cooling. This effect occurs because the signal and the noise travel in different directions inside the resonator, allowing only the signal of interest to be upconverted. Consequently, this lowers the effective temperature of the resonator below its physical temperature, potentially enabling applications without the need for cryogenics [6].

One crucial current limitation of this application is the efficiency of the various processes involved. A near 100% upconversion efficiency is essential for optimal performance. Additionally, it is imperative to enhance the Q factor to maximize the production of entangled photon pairs per second. Currently, significant research efforts are focused on reducing losses and enhancing fabrication procedures to increase the Q factor. Moreover, another critical area of research involves developing an idler storage solution that must be as lossless as possible.

In conclusion, the design outlined in this research holds promise for advancing the capabilities of small object detection using quantum illumination, particularly in spaceborne applications where power efficiency and compactness are crucial. Leveraging the features of photonic integrated whispering gallery mode resonators and passive cooling, this design presents a compelling solution for addressing the challenges of weak signal power detection. However, it is crucial to acknowledge that overcoming current limitations, such as achieving higher upconversion efficiency and enhancing the Q factor, requires continued research and development efforts.

REFERENCES

[1] A. Manis, J. A. Arnold, J. Murray, B. Buckalew, C. Cruz, y M. Matney, “An overview of ground-based radar and optical measurements utilized by the Nasa Orbital Debris Program Office”, *2nd International Orbital Debris Conference (IOC II),* 2023.

[2] Z. Zhang, S. Mouradian, F. N. C. Wong, y J. H. Shapiro, “Entanglement-enhanced sensing in a lossy and noisy environment”, *Phys. Rev. Lett*., vol. 114, num. 11, 2015.

[3] R. Assouly, R. Dassonneville, T. Peronnin, A. Bienfait, y B. Huard, “Quantum advantage in microwave quantum radar”, *Nat. Phys*., vol. 19, num. 10, pp. 1418–1422, 2023.

[4] S. Lloyd, “Enhanced sensitivity of photodetection via quantum illumination”, *Science*, vol. 321, num. 5895, pp. 1463–1465, 2008.

[5] G. Sorelli, N. Treps, F. Grosshans, y F. Boust, “Detecting a target with quantum entanglement”, *IEEE Aerosp. Electron. Syst. Mag*., vol. 37, num. 5, pp. 68–90, 2022.

[6] G. A. S. Botello, “Low noise thz detection via optical parametric upconversion”, Universidad Carlos III de Madrid, Spain, 2021.

[7] Sahu, Rishabh. “Cavity Quantum Electrooptics.” Institute of Science and Technology Austria, 2023.

[8] A. Rueda et al., “Efficient microwave to optical photon conversion: an electro-optical realization”, *Optica*, vol. 3, num. 6, p. 597, 2016.

[9] S. Barzanjeh et al., “Stationary entangled radiation from micromechanical motion”, *Nature*, vol. 570, num. 7762, pp. 480–483, 2019.

[10] S. Guha y B. I. Erkmen, “Gaussian-state quantum-illumination receivers for target detection”, *Phys. Rev. A*, vol. 80, num. 5, 2009.